



## AN IMPROVED DESIGN METHODOLOGY FOR SEISMIC ISOLATION SYSTEMS USING NONLINEAR RESPONSE SPECTRA

L. Jones<sup>(1)</sup>, I. Aiken<sup>(2)</sup>, C. Black<sup>(3)</sup>, D. Whittaker<sup>(4)</sup>, R. Retamales<sup>(5)</sup>, R. Boroschek<sup>(6)</sup>

<sup>(1)</sup> *President, Maxlide Ltd, Christchurch, New Zealand, linzjonz@maxlide.com*

<sup>(2)</sup> *Principal, Seismic Isolation Engineering, Inc., Emeryville, California, USA, ida@siecorp.com*

<sup>(3)</sup> *Associate, Seismic Isolation Engineering, Inc., Emeryville, California, USA, black@siecorp.com*

<sup>(4)</sup> *Technical Director, Structural, Beca Ltd, Christchurch, New Zealand, david.whittaker@beca.com*

<sup>(5)</sup> *Senior Structural Engineer, Ruben Boroschek & Associates, Santiago, Chile, rodrigo.retamales@rba-global.com*

<sup>(6)</sup> *President, Ruben Boroschek & Associates, Santiago, Chile, ruben.boroschek@rba-global.com*

### **Abstract**

The authors have recently developed a new and improved design methodology for seismic isolation systems. The approach uses nonlinear acceleration and displacement spectra that are developed for the fundamental seismic isolation system properties of characteristic strength and post-yield stiffness (which is referred to as characteristic stiffness, and expressed as an equivalent period). The methodology has been previously investigated for site-specific seismic designs in New Zealand, the U.S., Canada, and Turkey and this paper continues the development. The present study has two main objectives: first, to demonstrate the power and efficiency of the method in the preliminary design process for seismically-isolated structures through several illustrative design examples, and second, to further develop ADRS spectra and to explore their potential standardization to further streamline and improve the seismic isolation system design.

The ADRS methodology represents a valuable and intuitive visual tool to enable designers to quickly determine isolation system design parameters likely to be most effective for a given site and specific project structural design criteria, with the ability to rapidly identify the “trade-offs” of different isolation periods and yield values (characteristic stiffness and strength). The design process is directly based upon practical isolation design physical parameters (strength, or friction coefficient, and post-yield stiffness, or period). Selected examples are given and discussion provided to illustrate the benefits of the approach.

The further development and potential standardization of ADRS spectra for isolation system design is also explored as part of the current work, and this has been undertaken in the context of seismic design in Chile. In just the last five years, Chile has experienced three very large earthquakes, with  $M_w$  magnitudes of 8.2, 8.3 and 8.8. A broad set of strong ground motion records from these three major events was selected and ADRS isolation design spectra developed. The resulting spectra are compared with the seismic isolation design requirements of the Chilean code, NCh2745:2013. The set of spectra also presented the opportunity to investigate general response “patterns” in the ADRS plots, for the possibility of defining simplified ADRS plots for quick, preliminary design that do not require direct nonlinear analysis.

*Keywords: seismic isolation; design; spectra; nonlinear analysis*

## 1. Introduction

Common seismic isolation device technologies such as lead rubber bearings or concave slider bearings exhibit very full force–displacement hysteresis and are able to dissipate large amounts of seismic energy. This type of hysteretic behavior is often approximated as an equivalent linear system with secant stiffness and equivalent viscous damping.

The longer period of vibration and significant damping of an isolated structure result in substantially lower acceleration, and thus force and damage, response than if the structure were fixed base. The corresponding, often significant, displacements are accommodated in the isolation devices that are designed to sustain such large movements without damage.

The concept of nonlinear Acceleration Displacement Response Spectra (ADRS) was introduced by the authors [1, 2]. It was shown to be a valuable tool for structural designers to graphically define the seismic demand and effective operating point, in terms of base shear and isolation system displacement, of isolation system designs for a range of characteristic strengths and characteristic stiffnesses. The nonlinear ADRS are developed for the design suite of ground motion time histories. The ADRS are shown to provide a more direct and meaningful approach for the design process than linear, iterative methods.

The approximations inherent to, and the necessarily iterative design process required for the “effective (secant) stiffness-equivalent viscous damping” method is eliminated. The ADRS method conveniently, and directly, presents the inelastic seismic demands on isolated systems in graphical form and provides a highly intuitive tool for design.

The initial work by the authors [1, 2] explored the use of ADRS to understand the response behavior of single-degree-of-freedom nonlinear isolation systems to a suite of actual strong motion records from the Canterbury earthquake sequence. In subsequent papers [3, 4], the methodology has been applied to sites in Wellington (NZ), San Francisco (USA) – near fault, Vancouver (Canada) and two locations in Turkey (Zones 1 and 2). In each case, a suite of recorded ground motions, scaled to meet appropriate code and/or design requirements was used. A comparison with the common code method based “equivalent viscous damping” was also presented.

The extremely active Chilean seismic environment represents a unique opportunity to evaluate the response of seismic isolation systems to recorded, large-magnitude earthquake events and make a valuable addition to the growing ADRS database. Sets of records from three recent, larger than  $M_w$  8, earthquakes were used to compute ADRS spectra and study the response of isolation systems with a wide range of system characteristics. The investigation was undertaken for the as-recorded motions, and also for the motions scaled using both time- and frequency-domain techniques to code spectral design requirements.

## 2. ADRS Methodology

Isolation system response for the development of ADRS contours is determined through time-history analyses of a Bouc-Wen hysteretic single-degree-of-freedom (SDOF) oscillator to represent the nonlinear behavior of the isolation devices. The nonlinear equation of motion for the SDOF system was solved directly using Matlab [5], as described below.

Dynamic equilibrium of a general elasto-viscoplastic oscillator is given by

$$\ddot{u}(t) + \frac{F(t)}{m} = -\ddot{u}_g(t) \quad (1)$$

where  $u(t)$  is the relative-to-the-ground displacement history;  $\ddot{u}_g(t)$  is the ground acceleration, and  $F(t)$  is the internal force resulting from the restoring mechanism and damping (viscous or hysteretic). The internal force, assuming no contribution from viscous damping, can be expressed mathematically as

$$\frac{F(t)}{m} = \left(\frac{2\pi}{T_2}\right)^2 u(t) + \frac{Q_d}{W} g z(t) \quad (2)$$

where  $Q_d/W$  is the characteristic strength divided by the system weight,  $g$  is the acceleration of gravity;  $T_2$  is the isolated period; and  $z(t)$  is a hysteretic dimensionless quantity with  $|z(t)| \leq 1$ , that is governed by

$$u_y \dot{z} + \gamma |\dot{u}(t)| |z|^{n-1} + \beta \dot{u}(t) |z|^n - u(t) = 0 \quad (3)$$

where  $\beta$ ,  $\gamma$  and  $n$  are dimensionless quantities that control the shape of the hysteretic loop. The model given by Eqs. (2) and (3) is a version of the Bouc-Wen model [6, 7 and 8].

Substitution of Eq. (2) into Eq. (1) gives

$$\ddot{u}(t) + \left(\frac{2\pi}{T_2}\right)^2 u(t) + \frac{Q_d}{W} g z(t) = -\ddot{u}_g(t) \quad (4)$$

where  $z(t)$  is governed by Eq. (3). For the analyses performed for this study, it was assumed that the elastic stiffness is 100 times greater than the characteristic stiffness and therefore the problem is completely characterized by the isolated period,  $T_2$  and the ratio of characteristic strength to system weight,  $Q_d/W$ . For each combination of the characteristic strength and isolated period, the differential equations given by Eqs. (3) and (4) are solved simultaneously to obtain maximum displacement and corresponding acceleration for each ground motion considered.

### 3. Chilean Earthquakes and Seismic Isolation

Chile is one of the countries with the highest seismic activity in the world, primarily due to the subduction process of the Nazca Plate below the South American continent. This subduction process gives rise to different types of earthquakes, which are classified as inter-plate earthquakes (occurring in the contact zone between the Nazca Plate and the South American Plate), intermediate depth and large depth intra-plate earthquakes (occurring within the interior of the Nazca Plate), and shallow intra-plate earthquakes (occurring in the continental crust of the South American Plate). From the late 16<sup>th</sup> century to the present, there has been a high-magnitude ( $M_w > 7.5$ ) earthquake every 8 to 10 years on average throughout the Chilean territory.

The  $M_w$  8.8 Maule earthquake of February 27, 2010 caused economic losses exceeding 30 billion US dollars. A high percentage of these losses resulted from damage to nonstructural systems and components, such as architectural elements, building contents and electric and mechanical equipment. These huge losses, in addition to the public's perception regarding the earthquake's impact on property, have encouraged investors and real estate developers to incorporate seismic protection systems into buildings in order to achieve higher performance targets, that exceed the levels of current Chilean national codes. With almost 130 applications, seismic isolation is the seismic protection system that has experienced the most growth since 2010. Isolation is being used to protect critical and strategic infrastructure and structures with high-value contents, including hospitals, datacenters, museums, government buildings and emergency response facilities, and is seeing particularly, widespread adoption for both residential and office buildings.

### 4. ADRS for Recent Chilean Earthquakes

Seven pairs of ground motions recorded in the 2010  $M_w$  8.8 Maule earthquake, obtained from the Department of Civil Engineering at the University of Chile, eight pairs of ground motion records from the 2014 Iquique  $M_w$  8.2 earthquake, and six pairs of records from the 2015 Illapel  $M_w$  8.3 earthquake (both from the National Seismological Center of Chile) were used in the study. The records were selected for both soft and stiff soil sites and all were filtered using the NGA procedure, with the following steps: a. visually reviewed for instrument errors, b. baseline corrected, and pre-events removed, c. Fourier spectra evaluated for frequency content and cut-off frequency, d. tapering was applied to the ends of the records, and e. a Butterworth filter was applied. Five percent-damped acceleration and displacement response spectra for the three sets of processed earthquake ground motions are shown in Figs. 1 to 3.

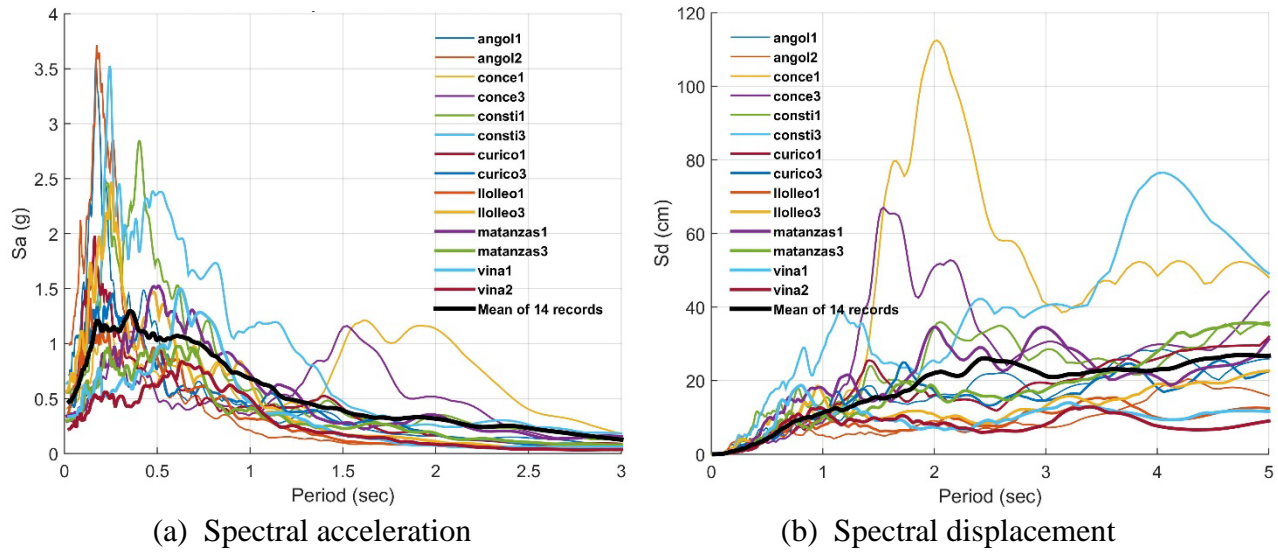


Fig. 1. Response spectra, Maule 2010, 14 records.

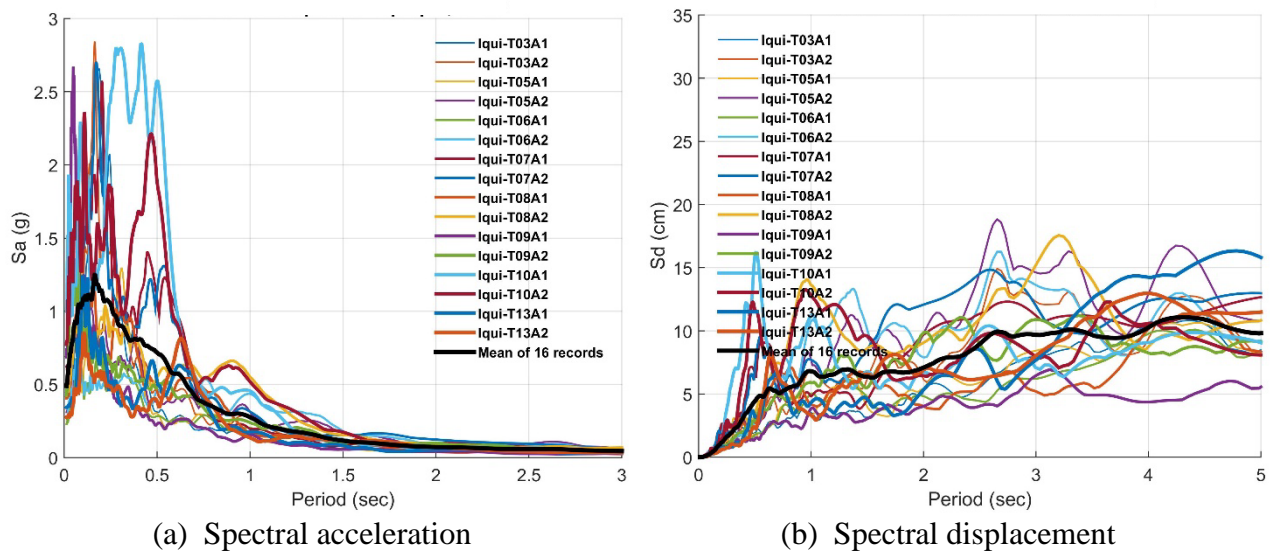


Fig. 2. Response spectra, Iquique 2014, 16 records.

ADRS plots were developed for each set of earthquake records, and also for the entire, combined suite (three sets) of records for the three earthquakes. Further, analyses were performed, and plots developed for (i) the as-recorded, unscaled motions, (ii) the three sets of records each scaled to the MCE design spectrum as defined in Chilean standard NCh2745:2013 for seismic isolation [9], and using the scaling methodology defined in NCh2745:2013 (which is the same procedure as defined in ASCE 7:10 [10] for seismic isolation design), and (iii) the three sets of records each frequency-scaled to the MCE spectrum of NCh2745:2013 in the period range from 0.01 to 10 seconds. Selected ADRS results for these three scaling conditions (i, ii and iii) are presented in the following sub-sections.

ADRS plots were developed for isolation periods of  $T_2 = 2, 3, 4$  and 5 seconds, and characteristic strengths of 4%, 6%, 8% and 10% of  $W$ . In all cases, the following ADRS plots show the mean of the SRSS of the response for each pair of ground motions from a recording station.

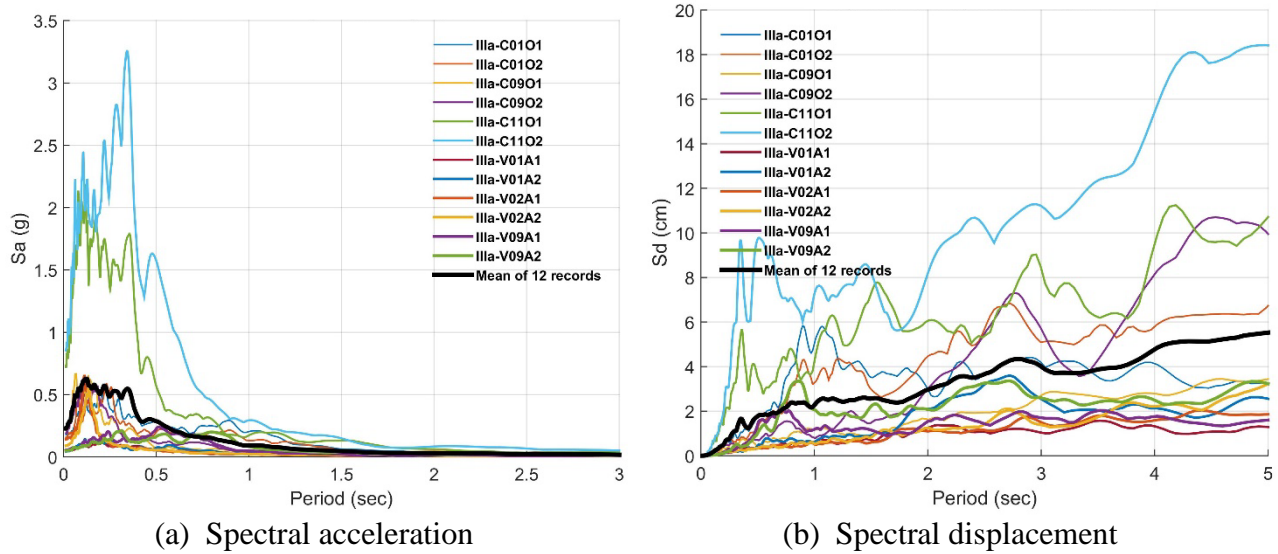


Fig. 3. Response spectra, Illapel 2015, 12 records.

#### 4.1 Maule, February 27, 2010, $M_w$ 8.8

The seven pairs of unscaled records for the Maule earthquake are the strongest of the three sets of motions in this study. Among the 32 records obtained in the earthquake, the most notable and unusual are the motions recorded at the Concepcion Centro station. This record had significant energy content around two seconds period (see Figs. 1(a) and 1(b)), attributed to a number of factors including the free vibration of deep soft soil deposits at Concepcion City which caused significant damage to tall buildings and long-period structures in Concepcion [11]. The response of isolation systems to the Concepcion record is dominant for the set of Maule records, and for this reason the ADRS contours for Maule are evaluated for the set of records both including, and excluding the Concepcion record. The ADRS plots for the unscaled Maule records are shown in Fig. 4. Fig. 4(a) shows the ADRS for the seven records including Concepcion, with displacements of about 130 to 350 mm for the range of isolation systems evaluated, while Fig. 4(b) shows the ADRS for the six pairs of records, not including Concepcion, and the range of displacements is only about 75 to 140 mm. The isolation system displacements indicated in Fig. 4(b) are consistent with displacements observed in isolated structures affected by the 2010 Maule earthquake, which were in the range of about 80 to 150 mm.

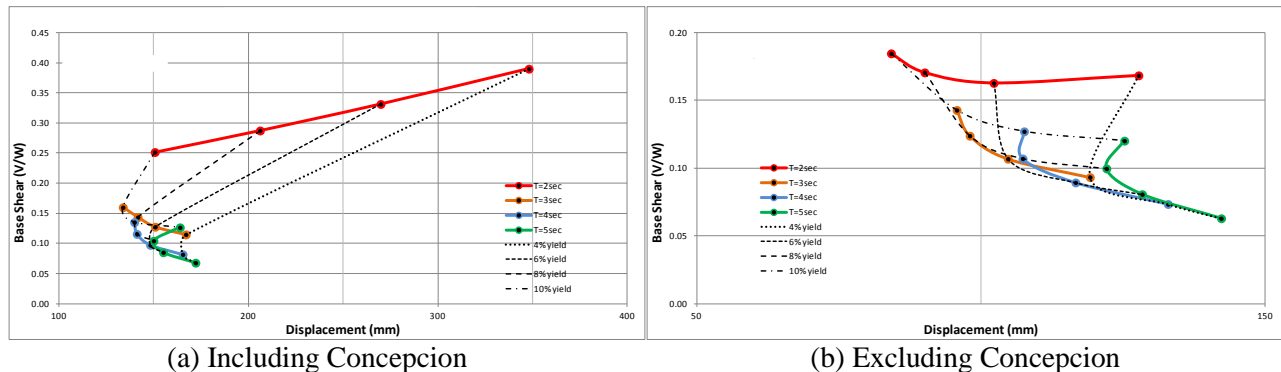


Fig. 4. ADRS contours, Maule 2010, 7 pairs of records, unscaled.

A constant scale factor of 1.85 was applied to scale the set of records to the NCh2745:2013 MCE spectrum. Fig. 5 shows the ADRS contours for the constant scale factor set of records, and Fig. 6 shows the ADRS contours for the frequency-scaled set of records.



In Figs. 5 and 6 differences between the results obtained using the two alternative scaling procedures can be observed. When the Concepcion recorded is excluded from the analysis, the type of scaling (constant, or time-domain, vs. frequency) does not have a significant influence on the ADRS contours, however, if Concepcion is included the constant scale factor approach results in larger displacements and base shears than given by frequency-domain scaling. Frequency scaling is believed to yield more appropriate results for design given that single scaling factors may result in excessive energy content at high frequencies, which controls elastic response and therefore the “initial conditions” for nonlinear behavior. The nonlinear behavior is also controlled by the initial stiffness and viscous damping of the system, variables not addressed in this paper. The information presented in the ADRS charts is therefore believed to be an upper bound estimate of system response.

Comparing Figs. 4 and 6, the displacement and base shear responses for the unscaled ground motions are about half of those given by the frequency-scaled records. For the set of records excluding Concepcion, whether for constant scale factor scaling or frequency-domain scaling, the responses indicated for isolation systems of 3 seconds period or longer are in the range of typical current Chilean design values.

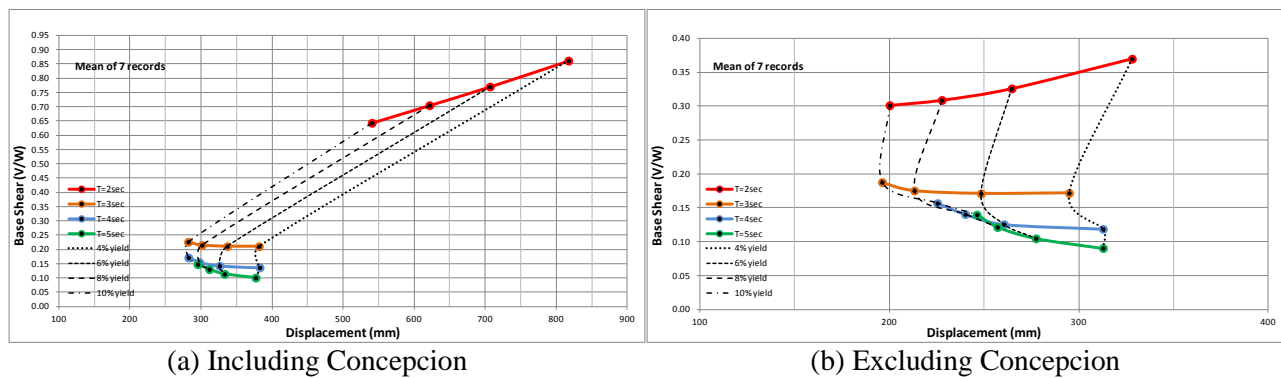


Fig. 5. ADRS contours, Maule 2010, 7 pairs of records, constant scale factor (x 1.85).

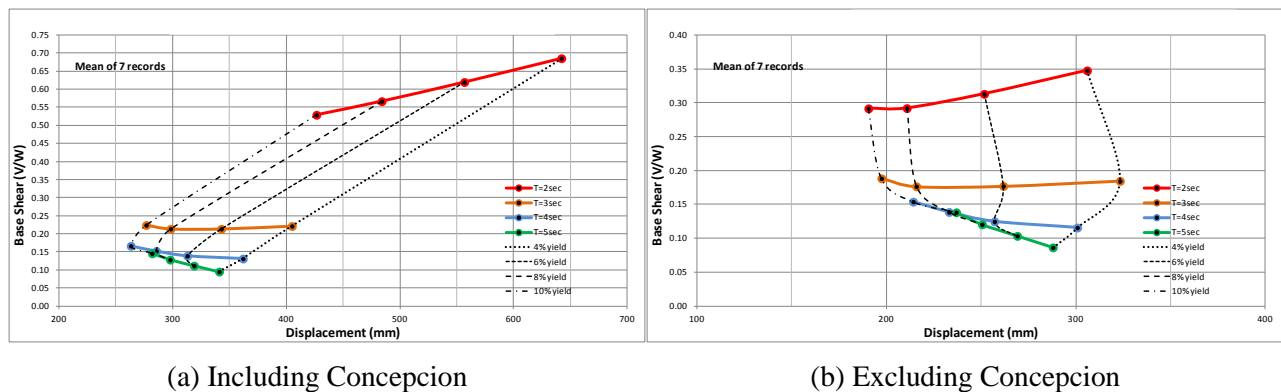


Fig. 6. ADRS contours, Maule 2010, 7 pairs of records, frequency scaled.

#### 4.2 Iquique, April 1, 2014, $M_w$ 8.2

The eight pairs of unscaled records for the Iquique earthquake do not cause significant seismic isolation system displacements; the ADRS plot (not presented) for the unscaled records shows displacements of only about 40 to 75 mm for the range of isolation systems evaluated. A constant scale factor of 6.2 was applied to scale the set of records to the NCh2745:2013 MCE spectrum. Fig. 7 shows the ADRS contours for the constant scale factor set of records, and Fig. 8 shows the ADRS contours for the frequency-scaled set of records.

For the scaled Iquique records, the ADRS contour trends, with regard to constant scale factor versus frequency-domain scaling, and also comparison with current Chilean design values, are essentially similar to those noted above for the Maule earthquake records.

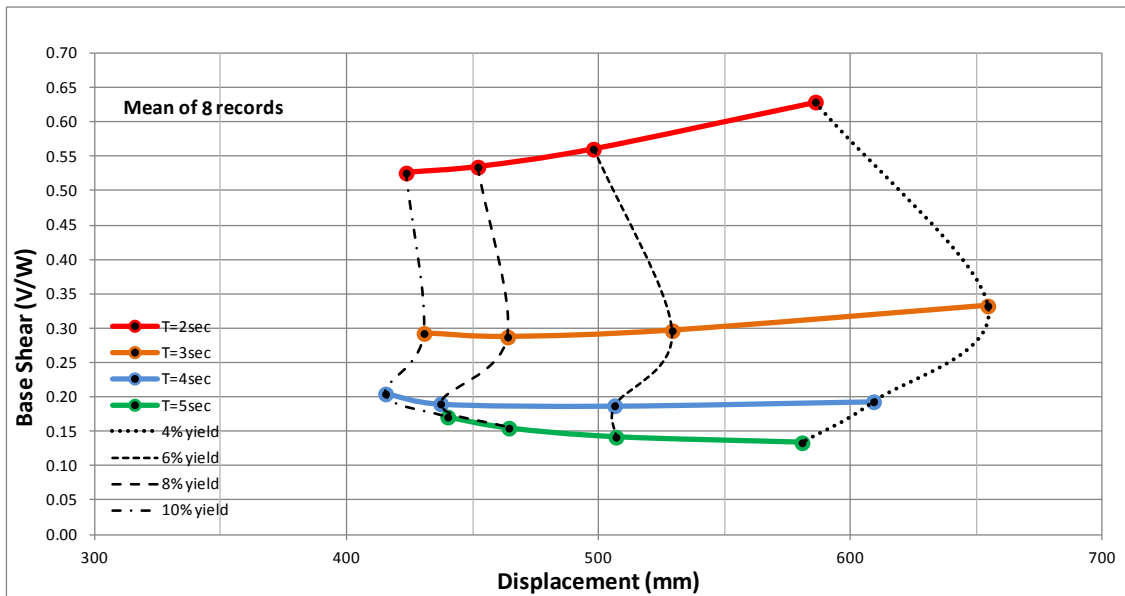


Fig. 7. ADRS contours, Iquique 2014, 8 pairs of records, constant scale factor (x 6.2).

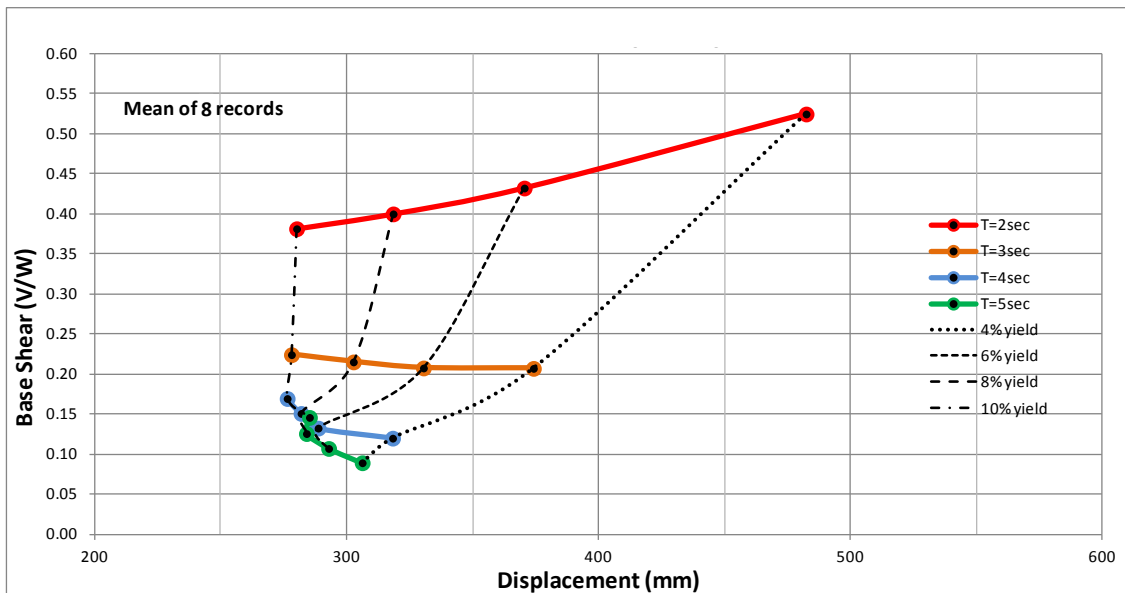


Fig. 8. ADRS contours, Iquique 2014, 8 pairs of records, frequency scaled.

#### 4.3 Illapel, September 16, 2015, $M_w$ 8.3

The six pairs of unscaled records for the Illapel earthquake are the least strong of the sets for the three earthquakes, and the largest constant scale factor (17.0) was required to scale the set of records to the NCh2745:2013 MCE spectrum. The ADRS plot (not presented) for the unscaled records shows displacements of only about 15 to 35 mm for the range of isolation systems evaluated. Fig. 9 shows the ADRS contours for the set of records scaled by a constant scale factor, and Fig. 10 shows the ADRS contours for the frequency-scaled set of records.

When comparing the constant scale factor and frequency-domain scaling ADRS contours of Figs. 9 and 10, respectively, some notable differences can be observed. In particular, the constant scale factor set of records indicate some large displacements, which are significantly larger than design values, and which are primarily attributed to the very large constant scale factor (17.0) applied.

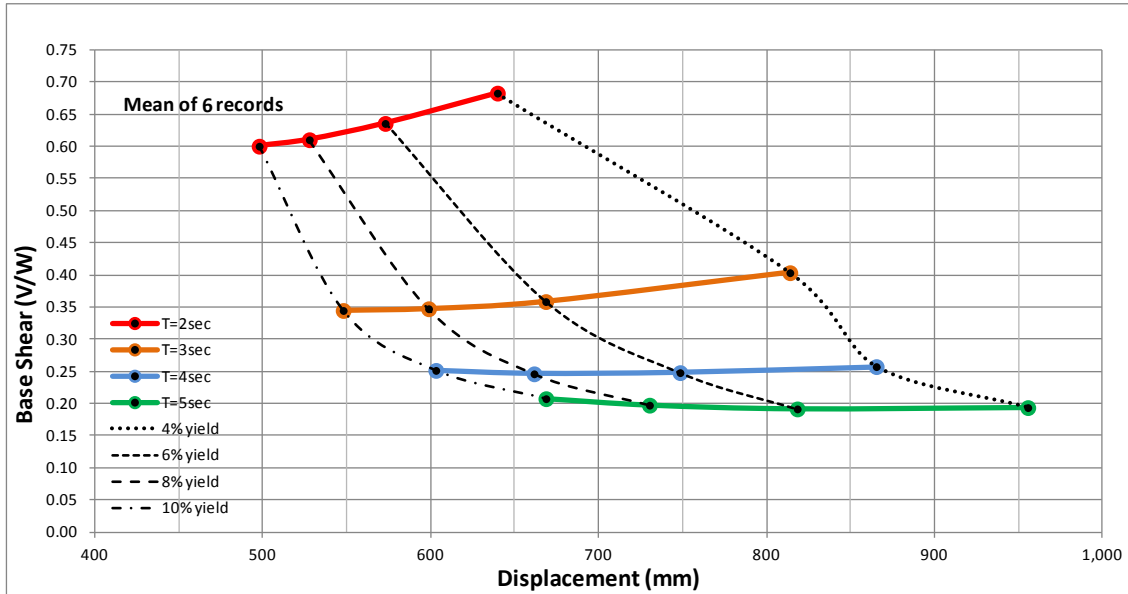


Fig. 9. ADRS contours, Illapel 2015, 6 pairs of records, constant scale factor (x 17.0).

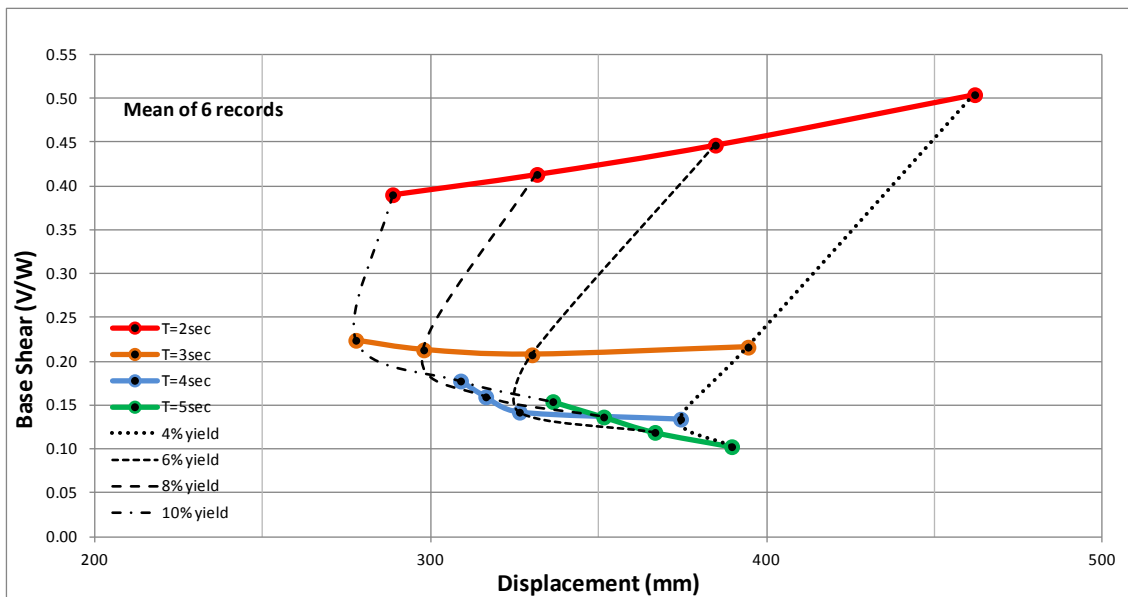


Fig. 10. ADRS contours, Illapel 2015, 6 pairs of records, frequency scaled.

#### 4.4 All records

ADRS plots for the combined set of ground motion records for all three earthquakes are shown in Figs. 11 and 12. Fig. 11 shows the ADRS plots for the combined set of single scale factor scaled motions, and Fig. 12 shows the ADRS plots for the combined set of frequency-scaled motions. In each figure, ADRS plots are shown for the (a) the combined set including the Maule Concepcion record, and (b) the combined set excluding the Concepcion record. As discussed above, the very significant spectral content in the Concepcion record at



approximately two seconds makes a dramatic contribution to the overall responses, and for this reason the combined set of records are evaluated both with and without Concepcion. This contribution can be clearly seen by comparing the 2-second (red line) response curves between the Fig 11 or Fig. 12 (a) and (b) ADRS plots.

As already mentioned, the ADRS for the frequency-scaled records (Fig. 12(b)) indicate isolation system displacements and base shears that are in the range of typical Chilean design values.

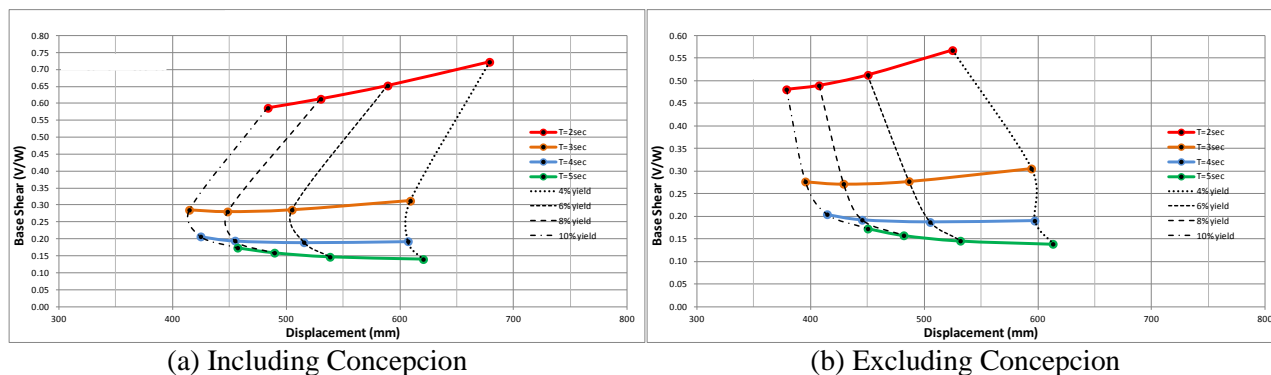


Fig. 11. ADRS for all records for three earthquakes, single-scale factor, including and excluding Concepcion

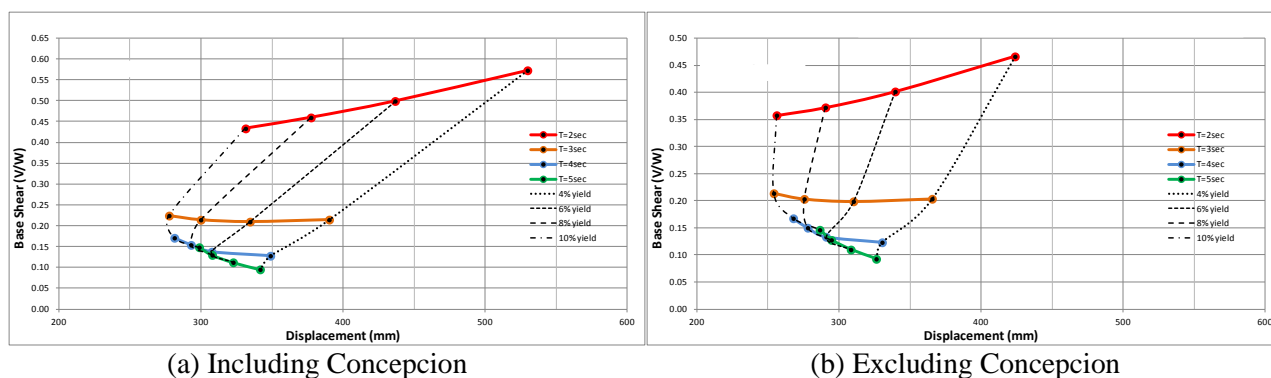


Fig. 12. ADRS for all records for three earthquakes, frequency scaled, including and excluding Concepcion

## 5. Conclusions

With readily available computational power and numerical tools, the development of the ADRS contours using a nonlinear time-history analysis methodology is quite feasible for the preliminary design of projects considering the use of seismic isolation. In the absence of nonlinear time-history analyses, system responses estimated by a code equivalent viscous damping approach can also be usefully expressed in this form.

The amplitude of the isolation system displacements indicated by the Maule ADRS contours are consistent with the displacements actually observed for isolated structures affected by the earthquake, which were in the range of 80 to 150 mm. For the sets of earthquake records studied, the constant scaled factor (time-domain) scaling method consistently results in larger isolation displacement and base shears than given by frequency-domain scaling.

The ADRS contours in Figs 11 and 12 show clearly the benefits of the ADRS approach of comparing the performance of isolation systems having different dynamic (period) and damping (yield) characteristics. Assuming that the frequency-scaled records provide more “accurate” results for design than do the time-scaled records, then it is clearly seen, in either Fig. 12(a) or 12(b) that a stiffer isolation system (for example, the red, 2-second line) exhibits both the highest base shear and displacement response, which is a response trend contrary to what most designers would expect. Thus, the ADRS charts enable the structural engineer to quickly and

effectively compare different available isolation system types or designs (and their associated cost and cost-benefit).

The use of ADRS contours based on characteristic isolation system parameters, whether by nonlinear time-history analysis or code-based equivalent viscous damping methods, represents a significant improvement over the preliminary design approach that has been widely prevalent to date, namely that based on 5%-damped linear elastic response spectra. The resulting charts provide a valuable and intuitive visual tool to enable designers to quickly determine isolation system design parameters likely to be most effective for a given site. The “trade-offs” of different isolation periods and yield values (characteristic stiffness and strength) can be clearly identified. Further, a rational basis for determining acceptable property variations (applicable for the design process, and also for device testing) is provided rather than relying on arbitrary code specified values. The general use of the ADRS methodology should greatly facilitate the rapid, and accurate preliminary design of isolation systems for projects, and will represent another advance in expanding the use of the technology.

Future work is intended: analyses to more thoroughly understand the effects of initial stiffness and damping on response, and, more generally, to continue the derivation of ADRS contours for an increasing number of ground motion suites for different locations and different seismic hazard levels, with the hope of moving in the direction of more general, long-term ADRS characterization for seismic isolation systems demands and designs.

## 6. Acknowledgements

The contributions of Felipe Guerrero, particularly the OpenSees analyses for some of the ADRS spectra, are gratefully acknowledged.

## 7. References

- [1] Whittaker, D. and Jones, L. (2013): Design spectra for seismic isolation systems in Christchurch, N.Z. *NZSEE Annual Technical Conference*, Auckland, New Zealand.
- [2] Whittaker, D. and Jones, L. (2014): Displacement and acceleration design spectra for seismic isolation systems in Christchurch, N.Z. *NZSEE Annual Technical Conference*, Wellington, New Zealand.
- [3] Jones, L., Aiken, I., Black, C. and Whittaker, D. (2015): Design displacement and acceleration spectra for seismic isolation systems. *14<sup>th</sup> World Conference on Seismic Isolation, Energy Dissipation and Active Vibration Control of Structures*, San Diego, California, USA.
- [4] Jones, L., Aiken, I., Black, C., Whittaker, D. and Sadan, B. (2015): Nonlinear response spectra for isolation system design: case studies in Turkey, California and New Zealand. *3<sup>rd</sup> Turkish Conference on Earthquake Engineering and Seismology*, Izmir, Turkey.
- [5] Mathworks (1992): Matlab high-performance numeric computation and visualization software. The MathWorks, Natick, Massachusetts.
- [6] Wen, Y-K. (1975): Approximate method for nonlinear random vibration. *J. of Engrg. Mech.* **102**(EM4): 389-401, American Society of Civil Engineers.
- [7] Wen, Y-K. (1976): Method for random vibration of hysteretic systems. *J. of Engrg. Mech.* **102**(EM2): 249-63, American Society of Civil Engineers.
- [8] Makris, N. and Black, C. (2004): Dimensional analysis of bilinear oscillators under pulse-type excitations. *J. of Engrg Mech.* **130**(9): 1019-31. ASCE.
- [9] National Institute of Standards (2013): Analysis and design of buildings with seismic isolation, *Chilean Standard NCh2745:2013*, Santiago, Chile.
- [10] ASCE. (2010): Minimum Design Loads for Buildings and Other Structures, *ASCE/SEI 7-10*, American Society of Civil Engineers.



[11] Saragoni, R., Ruiz, S., Madariaga, R., et al. (2012): Terremoto en Chile  $M_w=8.8$ , 27 de Febrero de 2010. Department of Civil Engineering, Physical and Mathematical Sciences School, University of Chile.